

Designing patient-specific 3D printed craniofacial implants using a novel topology optimization method

Alok Sutradhar^{1,2} · Jaejong Park² · Diana Carrau¹ · Tam H. Nguyen³ · Michael J. Miller¹ · Glaucio H. Paulino⁴

Received: 31 July 2013 / Accepted: 11 November 2015 / Published online: 11 December 2015
© International Federation for Medical and Biological Engineering 2015

Abstract Large craniofacial defects require efficient bone replacements which should not only provide good aesthetics but also possess stable structural function. The proposed work uses a novel multiresolution topology optimization method to achieve the task. Using a compliance minimization objective, patient-specific bone replacement shapes can be designed for different clinical cases that ensure revival of efficient load transfer mechanisms in the mid-face. In this work, four clinical cases are introduced and their respective patient-specific designs are obtained using the proposed method. The optimized designs are then virtually inserted into the defect to visually inspect the viability of the design. Further, once the design is verified by the reconstructive surgeon, prototypes are fabricated using a 3D printer for validation. The robustness of the designs are mechanically tested by subjecting them to a physiological loading condition which mimics the masticatory activity. The full-field strain result through 3D image correlation and the finite element analysis implies that the solution can survive the maximum mastication of 120 lb. Also, the designs have the potential to restore the buttress system and provide the structural integrity. Using the topology optimization framework in designing the bone replacement

shapes would deliver surgeons new alternatives for rather complicated mid-face reconstruction.

Keywords Craniofacial reconstruction · 3D printed implants · Topology optimization · Bone replacement · Segmental bone defects

1 Introduction

Reconstruction of the maxilla and midfacial structures after trauma or tumor removal remains a challenging problem for reconstructive surgeons. An inherent difference exists between defects that are sustained during cancer ablation and those that result from trauma [19], but both are difficult to manage surgically because of the significant functional and aesthetic roles of the mid-face. In addition to obliteration of the defect, the issues of swallowing, orbital function, vision, mastication, speech, restoration of facial contour, and symmetry also need to be addressed [18]. Large bone segmental bone defects in the mid-face typically require bone transfer for a successful outcome, and advances in microvascular free flaps (i.e., contain both soft tissue and bone) have greatly increased reconstructive options. The most commonly used composite flaps include the osteocutaneous radial forearm fibula, iliac crest, and the subscapular system of flaps [2]. The surgical planning of osteotomies has been made easier through the advent and use of virtual surgical planning [14], stereolithography modeling and simulation, and prefabricated osteotomy bone cutting templates [3, 22, 37]. However, the issues revolving around vascularity, volume and skeletal support [29], bone stock for osseointegrated implants [8, 9], and maintenance of shape and reduced bone reabsorption still pose as challenges, and a lack of consensus in the optimal surgical management of maxillectomy defects remains.

✉ Alok Sutradhar
sutradhar.1@osu.edu

¹ Department of Plastic Surgery, The Ohio State University, Columbus, OH 43210, USA

² Department of Mechanical and Aerospace Engineering, The Ohio State University, Columbus, OH 43210, USA

³ Department of Civil and Environmental Engineering, Northeastern University, Boston, MA 02115, USA

⁴ School of Civil and Environmental Engineering, Georgia Institute of Technology, Atlanta, GA 30332, USA

Surgical outcome can be enhanced by taking an interdisciplinary approach. In fact, the foremost important step in reconstructive surgery is to design a bone replacement that would qualitatively fulfill the form, function, fixation, and formation [24], known as 4F in the literature. Currently, the clinical approach is to use free flaps, pedicle flaps, or prosthetic obturator with or without alloplasts or grafts [21]. However, using tissue engineering techniques by combining the cells, biomaterials, and appropriate biochemical factors, a bone structure may be regenerated at the site using a background structure (known as ‘scaffold’). Bone replacement scaffold needs to properly fill the region of defect (form), bear the mechanical loading (function), be secured to surround tissue so that further loosening (pseudarthrosis) can be avoided (e.g., fixation) while it helps tissue formation by supporting nutrition transport and delivery (formation). Ideally, the scaffold should mimic the physical and chemical structures of the replaced tissue.

The optimal biomaterial which satisfies all the functional and safety requirement (e.g., stability, biocompatibility, no toxicity, intraoperative fitting, low cost, high production safety, low cost, low failure rate) is still remote. Primarily, biomaterials can be divided into two categories on how they are used: biomaterials for osteosynthesis and biomaterials as bone substitutes [32]. Historically, metals have been used for craniofacial applications which includes, stainless steel, vitallium, and metal alloys [15]. Titanium and titanium-based alloys have been widely used in different areas of orthopaedics implants. Titanium has a much lower elastic modulus compared to stainless steel and cobalt-chrome. Titanium-based implants have shown better performance due to their higher strength to weight ratio, biocompatibility, osteointegration, durability, and also better corrosion resistance. However, even in titanium-based implants, the disparity of the elastic modulus between the titanium and the bone results in stress shielding (the modulus of titanium is almost six times more than that of cortical bone). The stress shielding causes bone atrophy and the bone degenerates leading to eventual fracture in the region surrounding the implant [15]. One way to minimize the disparity between the material properties of the bone and its surrounding is match the mechanical properties and the stiffness. By inserting pores in the titanium implants, the elastic modulus of the material can be reduced and bring closer to bone [4, 36]. Using 3D printing and rapid prototyping techniques titanium implants with desired porosity can be pre-designed which are also tailored for wall thickness, pore size, and bulk modulus. Reconstruction of bone parts can be restored for minor defects using bone blocks, mesh bents with bone substitutes. Recently, using computer-aided design/manufacturing (CAD/CAM) techniques, cutting guides are being used to integrate virtual surgical planning with the real surgery showing good accuracy and promise [13, 21]. No matter what the material is,

the bone replacement needs to distribute the load efficiently without failure. In this work, we focus on the load distribution of the bone replacement structures.

Topology optimization is a structural optimization technique that gives the optimal topology of a structure that is subject to prescribed boundary and loading conditions. Optimal topology is obtained by assigning the best density values into each element in the discretized domain. The task is achieved by utilizing combination of a numerical method (e.g., finite element method) and an optimization algorithm. This technique is capable of showing locations where material is necessary and how to connect them to form a macrostructure. In this work, topology optimization is employed to design optimized shapes that will replace the region where bone loss occurred. The goal is to find the topology that would optimally handle combination of the load and boundary conditions such as supports from uninjured portions of facial skeleton and forces for mastication as well as cavities for nasal passageway and speech.

Topology optimization can be considered as guidance that aids achieving objectives of the aforementioned 4Fs of reconstructive surgery. Using topology optimization to design microstructures that enhances formation requirement with different pore sizes, hierarchical scaffold has been studied [1]. In order to improve the biomechanical environments, various material properties such as elasticity that matches bone, bulk modulus and diffusivity, and anisotropy of bones were proven to be crucial as well [25, 26]. Consideration of mechanical variables such as proper load transfer mechanism within a structure, biological factor such as vascularization for bone formation, and functional aspects such as providing proper platform for dental rehabilitation may be required to successfully accomplish the objective [39]. In a topology optimization framework, all of these variables can be included in the objective function. In our previous work [39], we demonstrated a ‘proof of concept’ by introducing topology optimization as a method for designing segmental bone replacements for simulated mid-face defects. Patient-specific simulation and virtual planning of the interventions using sophisticated numerical modeling and by use of advanced 3D printing (also rapid prototyping, stereolithographic modeling) can enhance the optimization of the treatment and improve the quality of life for the patient.

This paper suggests a new workflow to design patient-specific bone replacements for four different clinical defects based on classification of maxillary defects and studies to see the effect of different topological configuration in the optimization framework. The feasibility of the bone replacement forms is also examined by inserting them into the deformity regions using 3D CAD principles. The CAD models are 3D printed, and their mechanical practicality is examined through simulation of typical mastication activity and experimental validation.

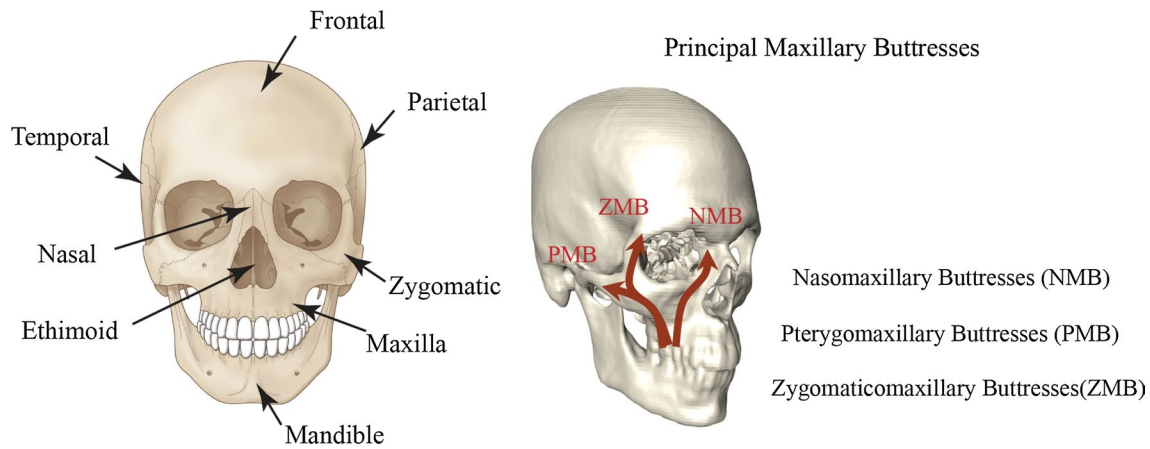


Fig. 1 Human skull anatomy and principal maxillary buttresses

2 Materials and methods

This section describes the aspects of craniofacial anatomy and buttresses, functional requirements, and the maxillary defect classification which are the basis of selecting patient-specific cases, followed by the novel multi-resolution 3D topology method.

2.1 Craniofacial anatomy, buttress, and functional Requirement

The primary bones of the facial skeleton include the frontal bone, ethmoid, vomer, and mandible located down the midline and the zygomatic, maxillary, palatine, and nasal bones appearing bilaterally. The frontal bone constitutes the upper face, the zygomatic, maxilla, palatine, and nasal bones constitute the middle or mid-face, and the mandible the lower face. Important basic life functions such as vision, speech, mastication, swallowing, olfaction, and respiration depend on the integrity of these bones, as does a person's individual, unique appearance. Reconstruction of the facial skeleton is thus particularly challenging because the bones of the face have significant functional and aesthetic considerations.

The mid-face is responsible for maintaining a patent nasal passageway, supporting the ocular globe, and withstanding the forces of mastication. These forces are transmitted through structural pillars or buttresses within the facial skeleton [35]. There are three primary vertical buttresses in the face, two anterior and one posterior, which have been well described [17, 23, 28, 41]. They are the nasomaxillary buttress, the zygomaticomaxillary buttress, and the pterygomaxillary buttress (see Fig. 1). The role of buttress reconstruction in relieving stress on the facial skeleton has been shown to be critical after maxillectomy in order for the facial skeleton to withstand the strong forces

of mastication and other basic functional requirements [20, 31, 41]. Recreation of missing buttresses also makes it possible for the face to maintain its vertical height and horizontal width, and anterior projection.

The goals of mid-face reconstruction include wound closure, separation of oral and nasal cavities, restoration of functional dentition and mastication, speech, support and maintenance of ocular globe position, maintenance of a patent nasal airway, and restoration of facial appearance [18, 29]. Surgeons aim to achieve these goals by restoring missing components of the buttress system. Over the years, several defect classification schemes and treatment algorithms have been proposed, though none is universally accepted.

2.2 Maxillary defect classification

The algorithm to classify maxillary defects is generally based on extent of resection of the maxilla [10], with treatment options focused on meeting surface area and volume requirements of the defect [29]. The type I defect, or limited maxillectomy, includes resection of one or two walls of the maxilla, excluding the palate [10]. A type II defect, or subtotal maxillectomy, includes resection of the lower five walls of the maxilla with preservation of the orbital floor. A type III defect, also known as a total maxillectomy, includes resection of all six walls of the maxilla, with the orbital contents. A variety of grafts can be used to support the orbital contents in addition to recreating the missing buttresses in type III defects. Resection of the upper five walls of the maxilla and the orbital contents with preservation of the palate is categorized as a type IV defect, or orbitomaxillectomy. Another algorithm was proposed that categorizes maxillary defects into three major categories and dictates reconstruction of specific bony buttresses for each categorical defect [41]. A universally accepted maxillary

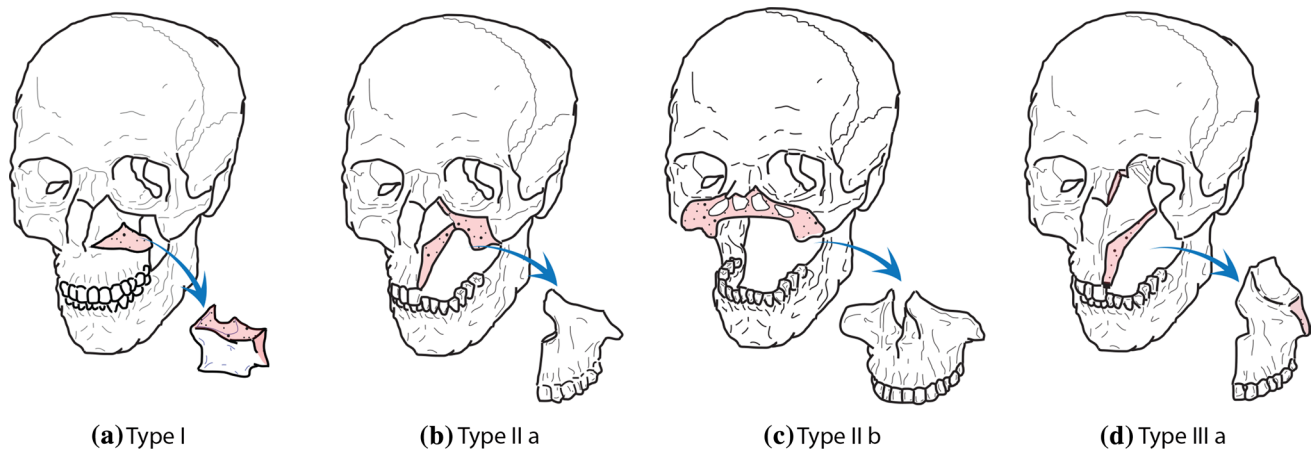


Fig. 2 Cordeiro maxillectomy classification

defect classification and algorithm for reconstruction remains elusive; for reviews, see [2, 7, 12].

No one algorithm can describe a defect and prescribe a treatment plan for all patients because maxillary defects are complex, with variable bony and soft tissue requirements. Surgical, prosthodontic, and patient factors can influence the choice of prosthetic versus surgical reconstruction [7, 8, 11, 16]. Factors such as a patient's age, associated diseases, degree of advanced carcinoma, preoperative and postoperative radiotherapy, and support for dental prosthesis affect the method of reconstruction [41]. Patients also have individual functional needs. Finite element analysis can supplement current reconstructive methods by creating osteotomy bone cutting templates that are structurally optimized and patient specific. In this paper, we deal four types of defects as shown in Fig. 2.

2.3 Topology optimization

2.3.1 Problem formulation

Topology optimization suggests the best material distribution within a design domain by seeking where to put the material (solid) and where not to (void). The topology can be defined by the density at different locations (e.g., pixels, voxel). The density is usually considered as a design variable and can assume an intermediate value between 0 and 1 with 0 representing the void and 1 representing the solid. The topology optimization used in this work optimizes the design variable which is the elemental densities in a design domain that would minimize the compliance (maximize the stiffness) of the final structure while satisfying the volume constraint. This objective function and constraints can be mathematically expressed as follows

$$\begin{aligned} \min_{\rho} C(\rho, \mathbf{u}) &= \mathbf{f}^T \mathbf{u} \\ \text{s.t. : } \mathbf{K}(\rho) \mathbf{u} &= \mathbf{f} \\ V(\rho) &= \int_{\Omega} \rho dV \leq V_s \end{aligned} \quad (1)$$

where C is the compliance, ρ is the density vector, \mathbf{f} is the global load vector, and \mathbf{u} is the global displacement vector. \mathbf{K} is the global stiffness matrix, Ω is the design domain, and V_s is the volume constraint. Employing the solid isotropic material with penalization (SIMP) method [5, 6], the problem is relaxed for density to have any value between 0 and 1 with small lower bound of $\rho_{\min} = 0.001$ to avoid singularities when calculating for equilibrium. That is,

$$0 < \rho_{\min} \leq \rho(x) \leq 1 \quad (2)$$

Also, with penalization power parameter (p) that is greater than 1, the intermediate density values are steered to either extreme and Young's modulus of each element is computed as follows

$$E(x) = \rho(x)^p E^0 \quad (3)$$

where E^0 is the Young's modulus of the material in the solid state (i.e., $\rho = 1$). The global stiffness matrix in Eq. 1 is calculated by summing up all the elemental stiffness matrices which depends on elemental density value ρ_e and takes the form of following

$$\mathbf{K}(\rho) = \sum_{e=1}^{N_{el}} \mathbf{K}_e(\rho_e) = \sum_{e=1}^{N_{el}} \int_{\Omega_e} \mathbf{B}^T \mathbf{D}(\rho_e) \mathbf{B} d\Omega \quad (4)$$

where $\mathbf{K}_e(\rho_e)$ is the stiffness matrix of the element e , \mathbf{B} is the shape function derivatives, and $\mathbf{D}(\rho_e)$ is the constitutive matrix which depends on the material density. Sensitivity

analysis is required for this gradient-based optimization problem. Sensitivities of the objective function and volume constraint with respect to design variable ρ_e are calculated as follows

$$\begin{aligned} \frac{\partial C}{\partial \rho_e} &= -\mathbf{u}_e^T \frac{\partial \mathbf{K}_e}{\partial \rho_e} \mathbf{u}_e = -p \rho_e^{p-1} \mathbf{u}_e^T \mathbf{K}_e^0 \mathbf{u}_e \\ \frac{\partial V}{\partial \rho_e} &= \int_{\Omega_e} dV \end{aligned} \tag{5}$$

where \mathbf{K}_e^0 is the stiffness matrix of element that is completely solid. (i.e., $\rho_e = 1$) and \mathbf{u}_e is the elemental displacement vector.

2.3.2 Efficient and accurate solution for topology optimization

The solution resolution depends on the meshing of the design domain. Better visualization and higher fidelity can be achieved by employing finer mesh for the design domain. However, with increased number of elements for computation, required CPU time gets longer with potential demand in parallel computing. This can be avoided by reducing computational cost directly with ‘fast iterative solvers’ to reduce the calculation time associated with finite element analysis [40]. Another approach to remedy higher computational cost is to take advantage of superelements. With relatively coarse mesh for displacement element, CPU time can be maintained low while relatively fine mesh of design variables provides enhanced visualization of the result.

Nguyen et al. [33] introduced an algorithm that utilizes multiple levels of mesh for topology optimization. The method called multiresolution topology optimization assigns coarse mesh for rather computationally expensive finite element analysis and finer mesh for design variable and density variable to enhance visualization. This approach is employed in this work and is detailed in the next section.

2.3.3 Multiresolution topology optimization

The multiresolution scheme in [33] is employed in this work to obtain high resolution solutions effectively. In an element-based topology optimization, displacement mesh coincides with design variable mesh thus single value represents the density of each displacement element. In the multiresolution scheme, different levels of meshes are used for each distinct purpose: displacement mesh for finite element analysis, design variable mesh for optimization, and density mesh for visualization. Typically, displacement mesh is relatively coarser than design and density mesh to save computational cost in the finite element analysis. Also,

minimum length scale and mesh independence in the result is guaranteed by using projection function on each design variables. This introduces following additional constraint to the original problem statement in Eq. 1.

$$\rho = f(\mathbf{d}) \tag{6}$$

where $f(\cdot)$ is the projection function and \mathbf{d} is the vector of design variables. Multiresolution scheme used in this work considers 3D problems and uses brick element with eight nodes for displacement mesh which is further discretized to have 125 uniform design variables and density elements ($B8/n125$). Assuming that density is uniform within density element, SIMP method yields following expression for elemental stiffness matrix

$$\mathbf{K}_e = \sum_{i=1}^{N_n} (\rho_i)^p \int_{\Omega_e} \mathbf{B}^T \mathbf{D}^0 \mathbf{B} d\Omega_e \tag{7}$$

where \mathbf{D}^0 is material property matrix corresponding to the solid state, and N_n is the number of density elements per displacement element. Sensitivity of elemental stiffness matrix is required for sensitivity analysis of compliance. Sensitivity of elemental stiffness with respect to design variable is calculated as follows

$$\frac{\partial \mathbf{K}_e}{\partial d_n} = \frac{\partial \mathbf{K}_e}{\partial \rho_i} \frac{\partial \rho_i}{\partial d_n} = \frac{\partial \sum_{j=1}^{N_n} (\rho_j)^p \mathbf{I}_j}{\partial \rho_i} \frac{\partial \rho_i}{\partial d_n} = (\rho_i)^{p-1} \mathbf{I}_i \frac{\partial \rho_i}{\partial d_n} \tag{8}$$

where

$$\mathbf{I}_i = (\mathbf{B}^T \mathbf{D}^0 \mathbf{B})|_{iA_i} \tag{9}$$

and d_n and ρ_i are the design variable and element density, respectively. The sensitivity analysis of the constraint is calculated similarly to Eq. 5 as follows

$$\frac{\partial V}{\partial d_n} = \frac{\partial V}{\partial \rho_i} \frac{\partial \rho_i}{\partial d_n} \tag{10}$$

2.3.4 Multiresolution topology optimization work flow

The topology optimization follows the workflow shown in Fig. 3. First, the information on the size and discretization of design domain needs to be input as well as boundary and loading conditions. Then, the optimization iteration is started with the initial density distribution ρ by finite element analysis to solve the equilibrium equation $\mathbf{K}(\rho)\mathbf{u} = \mathbf{f}$. Sensitivities are computed based on Eq. 8 through Eq. 10 followed by optional filter which modifies elemental sensitivities to remedy checkerboard pattern and alleviate mesh dependencies [6]. Optimization scheme is formulated based on the optimality condition obtained from the Lagrangian of Eq. 1. Appropriate move limit and damping coefficient are typically required to stabilize the convergence.

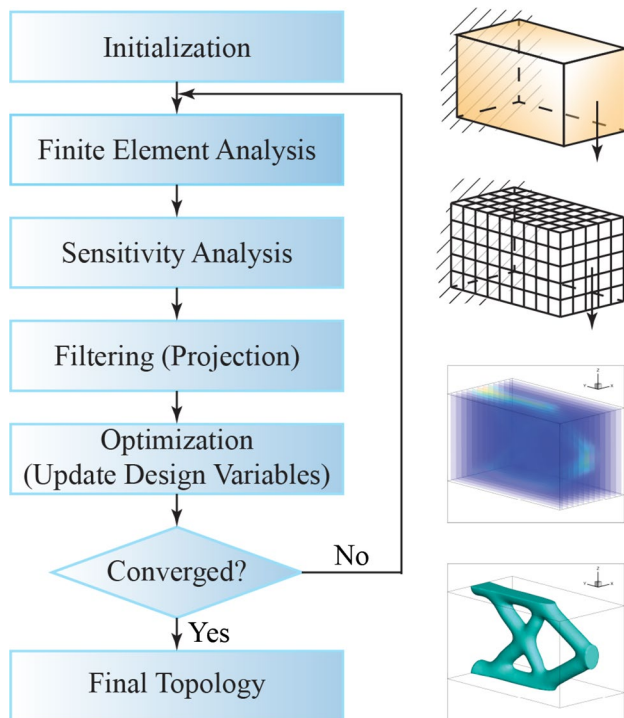


Fig. 3 Topology optimization flowchart

2.4 Model preparation

Topology optimization used in the work starts with a domain of a rectangular parallelepiped for 3D. Since the result of the topology optimization depends a lot on the domain geometry, choosing the right size of the domain is one of the most critical aspects in the technique. The multiresolution topology optimization scheme does not carry any length unit thus the ratios of the lengths in the

principal directions are considered to represent a design domain. Getting the proper domain size for a craniofacial defect starts with the computed tomography (CT) or the magnetic resonance image (MRI) of the patient. Appropriate threshold allows building isosurface by registering the skull from whole image data. Once the defect in the mid-face is exposed, 3D size of defect (length, width, and height) is measured using 2D or 3D measure tool. The domain is selected with the surgeon's insight in order to minimize the potential risk during the surgery and maximize the ease of implementation of the bone replacement. The other important input that controls the result in the algorithm is the boundary conditions. This includes information on where the loads and supports should be located. Desired cavity such as nasal passageway, eye cavity, or hard palate can also be taken into account.

2.5 Case studies based on maxillectomy classification

Four typical clinical cases are selected which represents actual examples of craniofacial defect created by cancer resection are shown in Fig. 4. Four patient data chosen for the study can be categorized as follows

- Case 1: Bilateral subtotal maxillectomy I
- Case 2: Bilateral subtotal maxillectomy II
- Case 3: Right limited maxillectomy
- Case 4: Left limited maxillectomy and mandibular defect in left lateral segment

The defect in case 1 is created in the center of mid-face and is asymmetrically extended bilaterally. According to the Cordeiro's maxillary defect classification [10],

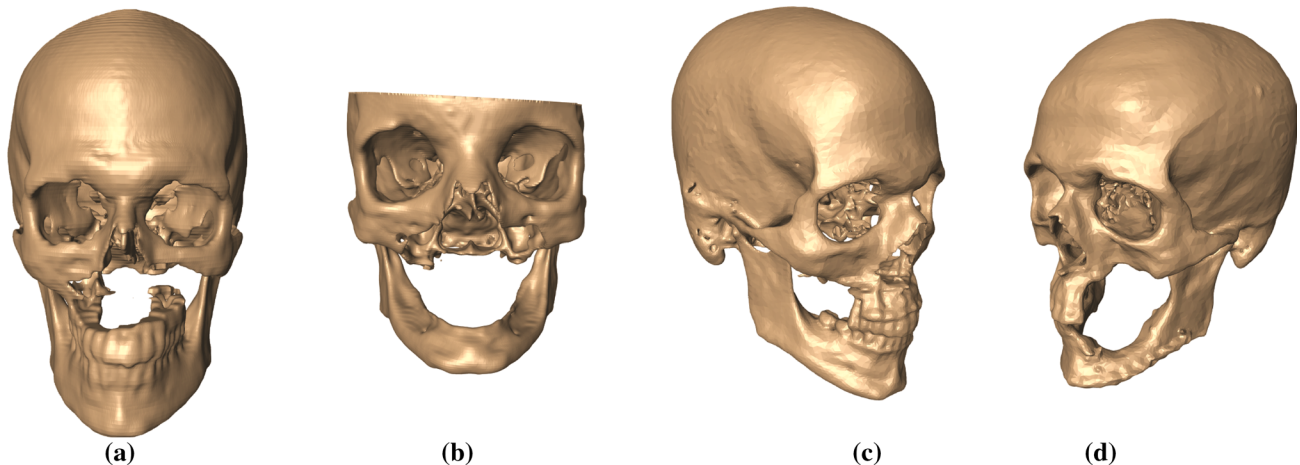


Fig. 4 Craniofacial skeletons of patients with severe mid-face defects: **a** Case 1: Bilateral subtotal maxillectomy I, **b** Case 2: Bilateral subtotal maxillectomy II, **c** Case 3: Right limited maxillectomy, **d** Case 4: Left limited maxillectomy and mandibular defect in left lateral segment

this case falls in type II as the orbital floors are still intact. The bone replacement shape for this defect has to have a bony structure that will connect the denture with orbital floor which ultimately replace the role of buttress system. Defect in case 2 is due to bilateral subtotal maxillectomy and is similar to that of case 1. Case 3 shows right limited defect thus is type I in Cordeiro's defect classification. Bone replacement shape for case 3 needs to provide a platform for missing molar teeth for enhanced symmetric mastication. Case 4 not only has mid-facial defect due to left limited maxillectomy but also has mandibular defect in the left lateral segment. In this case, two separate bone replacement shapes are required: one for the mid-facial defect that would provide a mechanism to transfer load (e.g., mastication) to the uninjured portion of facial skeleton and the other for mandibular defect that would support denture.

3 Results

In this section, we design bone replacements for the four clinical cases in Fig. 4 and present respective patient-specific designs using multiresolution topology optimization algorithm. First, we describe the Case 1 in great detail, analyzing the defect and discuss about the possible bone replacement shapes. Then, we present additional examples to validate the methodology.

3.1 Case 1: Bilateral subtotal maxillectomy I

This type of defect occurs typically due to trauma injuries (e.g, blast or gunshot wound) in the face or due to surgical removal of tumor which results in major loss of bone in the mid-face. This is a critical defect because the entire maxilla needs to be reconstructed. The patient has lost the capability of mastication or chewing. There is no dental activity in the upper region. In this case, all the three buttresses would have to be partially reconstructed and the loads from the teeth needs to be transferred to the adequate support. Finally, denture has to be inserted. In Fig. 5a, b, the region that is required to be reconstructed is depicted using a prismatic shape which is referred as 'design domain' in general. Based on the measurements from the image data, the domain size is selected to be $28 \times 20 \times 12$ (width, height, and depth, respectively). On the both sides, the edges of the zygomatic bone is where we expect the design domain will be supported using fixation screws. In Fig. 5b, the lateral support locations are inserted in those edges. As discussed earlier, primarily three different types of requirements need to be addressed, (1) functional, (2) structural, and (3) aesthetic. In order to ensure nasal air passage, a cylindrical cavity is placed in the design domain. This warrants that no material will be inserted in this region during the topology

optimization. Further, we have to account for the cavity inside the mouth that is bounded by the hard palate. As shown in Fig. 5b, a quarter ellipsoidal region is prescribed to account for this.

The general process during the topology optimization process is to put 'supports' on the lateral surfaces for the contact and the fixation between the bone replacement and the uninjured portion of the facial skeleton. In these locations, the multiresolution topology scheme assumes no displacement in finite element analysis step. A set of upward forces along reasonable teeth profile representing the mastication and another set of downward forces are provided on center of the top surface to simulate the trauma forces that may be transferred from the upper region of skeleton are included.

Based on the conditions shown in Fig. 5b, a total of 6720 ($28 \times 20 \times 12$) $B8 / n125$ elements are introduced in the multiresolution topology optimization scheme. The algorithm is allowed to take up to 12 % (V_s) of the total volume. A filter with size equal to 1 displacement element is employed. Unit forces are applied at the appropriate nodes of finite elements that discretize the design domain. The ratio of sum of downward forces on the top surface and the total upward forces along the teeth profile is 10. Maximum iteration is limited to 50. Solution from multiresolution scheme and a figure simulating surgical insertion is shown in Fig. 5c, d. In order to see the evolution of the solution, intermediate topologies in selected iterations are shown in Fig. 6. A quick visual inspection of the solution in Fig. 5c verifies that the embedded cavities are well incorporated. The design and the skull are then 3D printed to check the fit (see Fig. 5e). It should be noted that the result gives the topologically optimized structure for the set of load and boundary condition that is prescribed in the design domain. If the dimensions of the design domain, the load, the load ratio between upper and lower loads as well as the boundary condition change then a different optimized solution is going to be obtained. More material can be introduced into the optimized shape for other functionalities, for example fixation supports for prosthetic nose or denture and/or dental bars. In the next section, experimental validation using mechanical testing on this 3D printed implant embedded into the skull is presented for this defect.

3.2 Case 2: Bilateral subtotal maxillectomy II

Two different options are suggested for case 2 based on whether the masticatory forces have an additional component or not. For the first scenario, the domain size is chosen to be $32 \times 11 \times 20$. Supports are located on both the lateral surfaces. Unit mastication forces are applied in the teeth profile and assumed to be purely vertical and only nasal cavity is introduced. The depth is slightly increased in the

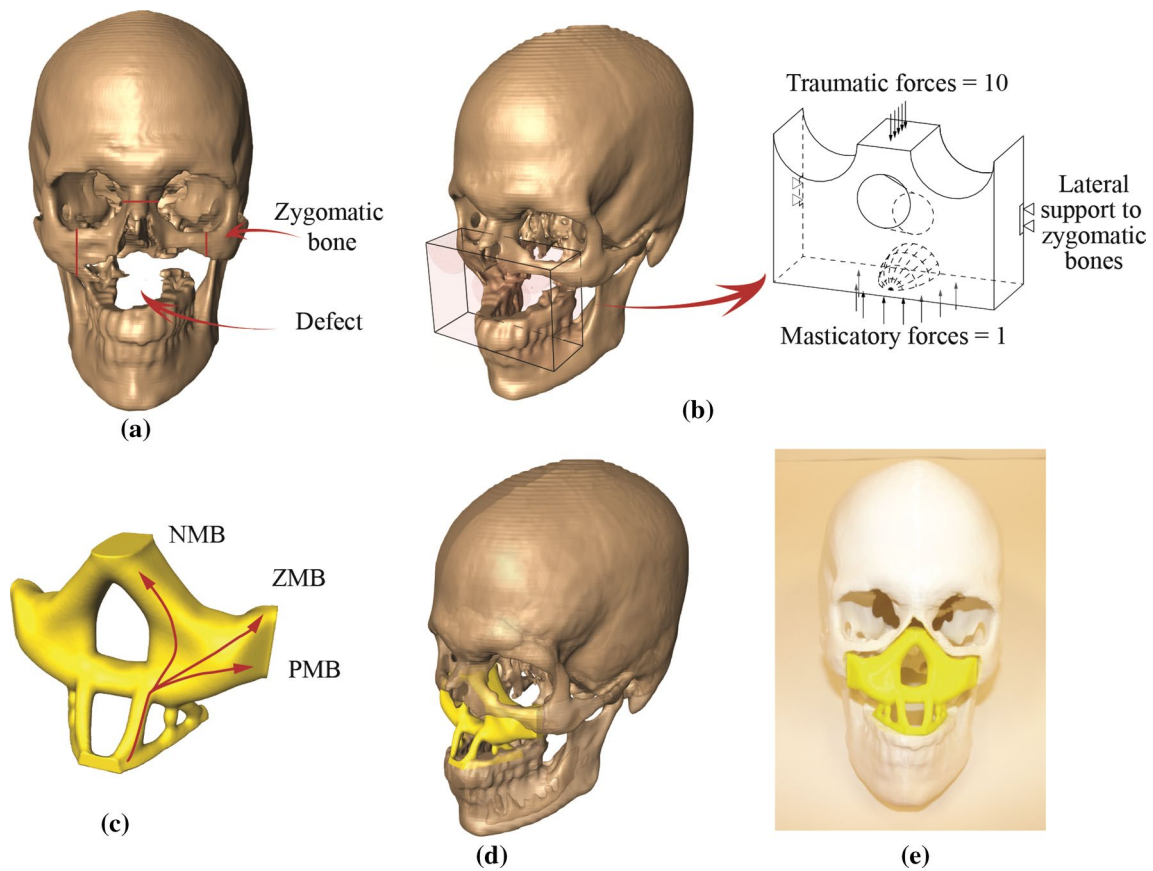


Fig. 5 Case 1: Bilateral subtotal maxillectomy I: **a** design domain, **b** boundary conditions, **c** bone replacement obtained from multiresolution topology optimization scheme depicted using an iso-surface ($\rho = 0.25$), **d** insertion simulation, **e** 3D printed skull model showing the final design fit

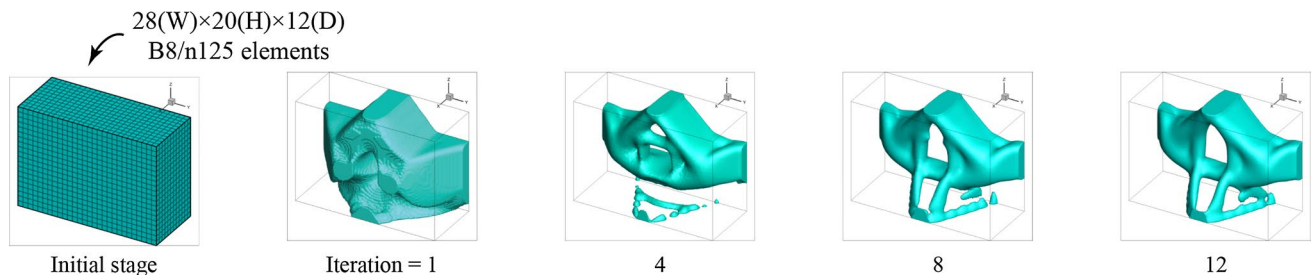


Fig. 6 Evolution of multiresolution topology optimization solution (intermediate topologies) for Case 1: Bilateral subtotal maxillectomy I

second scenario to be $32 \times 11 \times 25$. Masticatory forces in this scenario have additional horizontal component toward the center. The magnitude of horizontal component is 20 % of the vertical component. Nasal passageway and hard palate are embedded. The illustration of design domain and respective boundary conditions are shown in Fig. 7a, b. For both scenarios, volume fraction constraints (V_s) of 10 % are employed with all other design parameters remaining the same as in case 1. Solution from the multiresolution

scheme and the surgical insertion simulation are shown in Fig. 7c, d.

3.3 Case 3: Right limited maxillectomy

For case 3, the domain is chosen to be $6 \times 9 \times 17$. A support is provided on the posterior surface. Due to the rotated orientation of design domain, loads have vertical and horizontal components with a ratio of 1 between

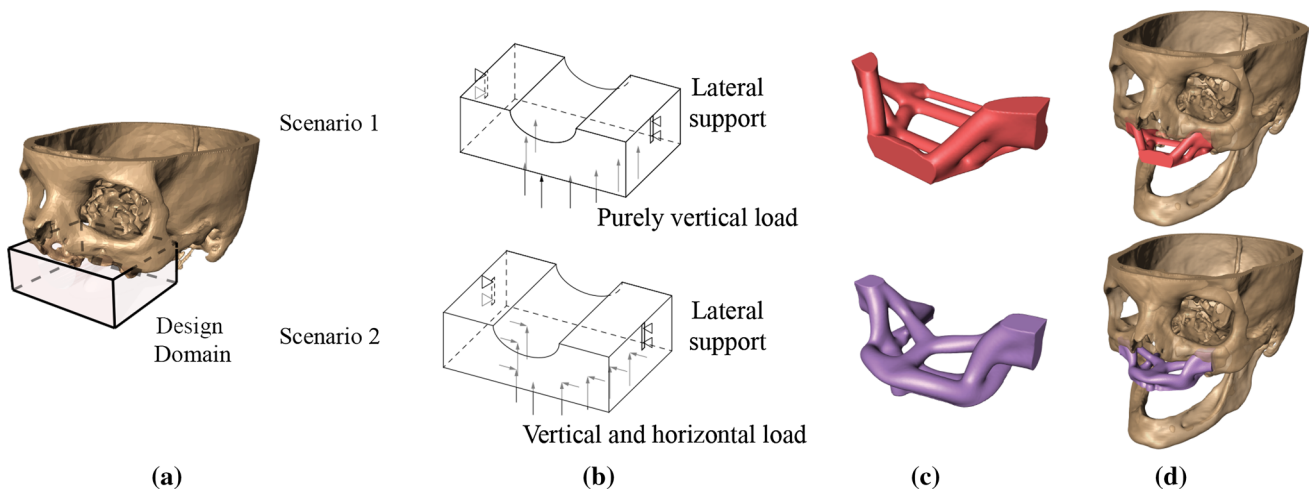


Fig. 7 Case 2: Bilateral subtotal maxillectomy II: **a** design domain, **b** boundary conditions, **c** bone replacement obtained from multiresolution topology optimization scheme depicted using an iso-surface ($\rho = 0.25$), **d** insertion simulation

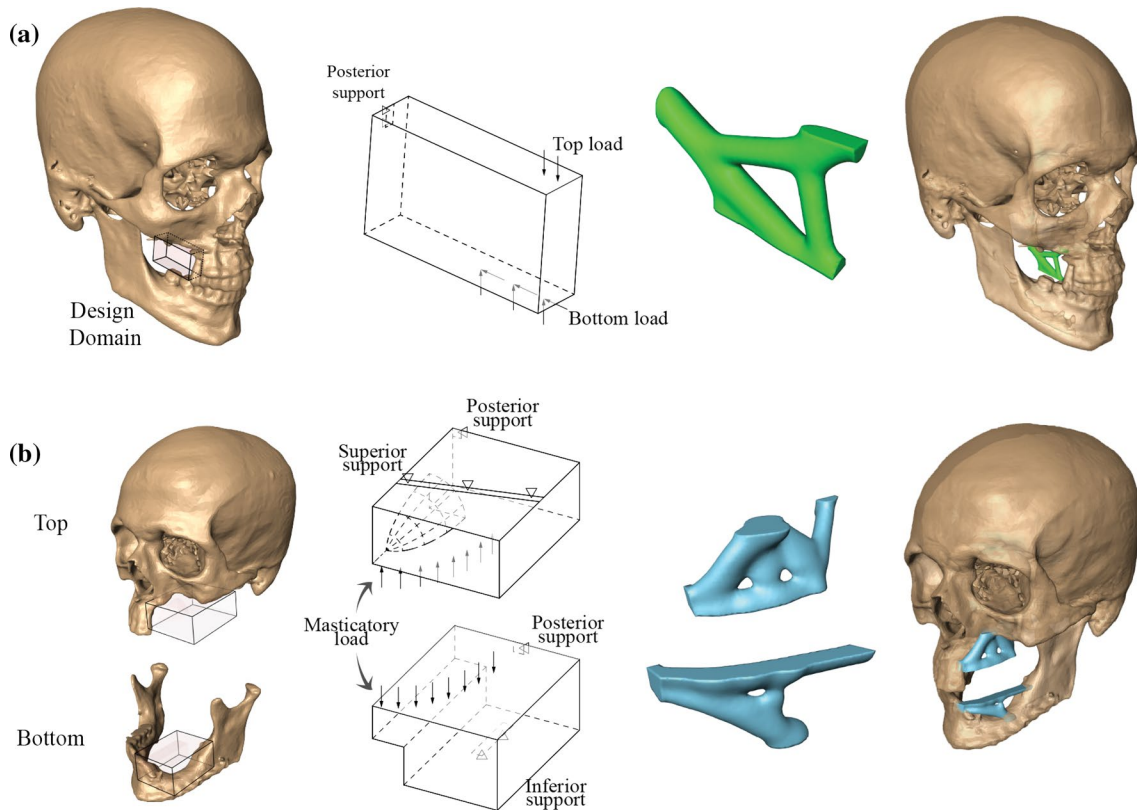
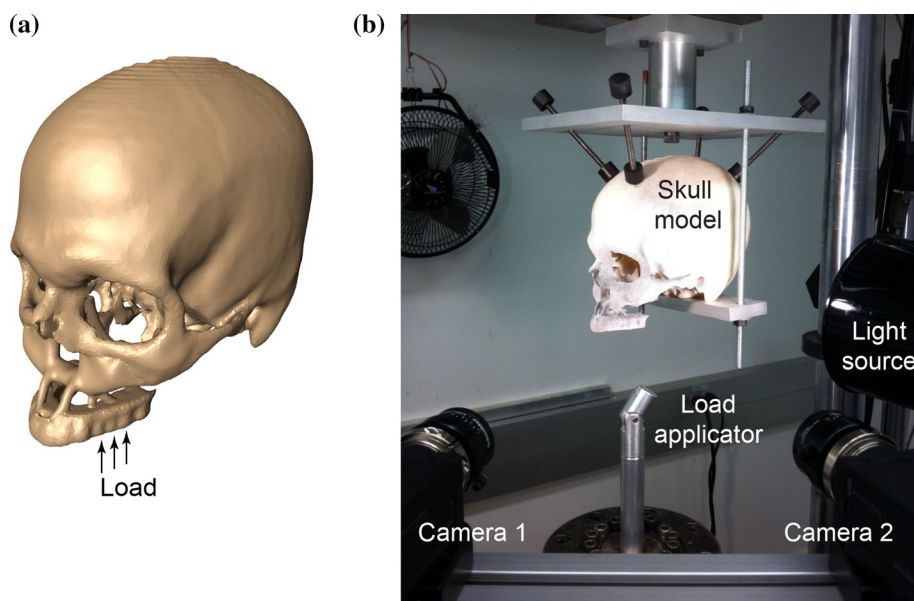


Fig. 8 Application of topology optimization scheme and solutions with iso-surface ($\rho = 0.25$) to **a** Case 3: Right limited maxillectomy, **b** Case 4: Left limited maxillectomy and mandibular defect in left lateral segment

them. A set of purely downward force is included on the top surface to ensure the connectivity between the top and the bottom surface. The design domain and the respective boundary conditions are shown in Fig. 8a. Employed design parameters are volume fraction constraint of

10 %, penalization factor (p) of 3. Filter radius equals the size of single displacement element. Implemented boundary condition along with the solution from the multiresolution scheme and the surgical insertion are provided in Fig. 8a.

Fig. 9 Simulation of mastication in the validation models: **a** CAD model, **b** setup for mechanical experiment on 3D printed model



3.4 Case 4: Left limited maxillectomy and mandibular defect in left lateral segment

Defect in the mid-face and in the mandible are separated in the design process with domain size of $15 \times 7 \times 18$ for the mid-face and $12 \times 7 \times 15$ for the mandible. Loads in this case are purely vertical on the teeth profile in both domains. Appropriate supports that would ensure contact with uninjured portion of facial skeleton are provided. For mid-face defect, a cavity that mimics hard palate is embedded. For both domains, volume fraction constraint of 5 % and penalization factor of 3 are selected. Aforementioned design domain, boundary conditions, design from multiresolution scheme, and simulation of surgical insertion are illustrated in Fig. 8b.

4 Design validation using mechanical testing on 3D printed implants

The mechanical performance and feasibility of topology-optimized solution is investigated using bone replacement design obtained for case 1. The design is placed in the region of defect using CAD software. The connections between uninjured portion of skull and solution are assumed to be fused to create single piece CAD model as shown in Fig. 9a. This validation model is then sent to a FDM (fused deposition modeling) 3D printer to be fabricated layer by layer using ABSplus TM-P430 thermoplastic.

Typical mastication activity is chosen to be simulated in the validation model. A distributed load is applied with

aluminum cylindrical load applicator over molar region on one side of validation model. A custom fixture is used to hold the validation model in place while the model is loaded from 5 lbs (preload) to 120 lbs (maximum load). The value of maximum load of 120 lbs is chosen because it is reported as the maximum masticatory force that human can generate [27]. Final configuration of the setup is provided in Fig. 9b.

During the testing, the mechanical behavior of the validation model is captured using 3D digital image correlation. This technique successively takes high resolution (1624×1224 pixels) images of the target and by correlating images it captures the deformation and calculates the full-field strain in the target.

Abovementioned mechanical testing is reproduced in the FEA package utilizing the material properties of the thermoplastic and same boundary conditions. The strain fields in the 3D printed validation model and in the FE model show good agreement with less than 6.2 % discrepancy which verifies validity of FE model for further analysis. Material property in the FEA is then changed to experimentally obtained human skull property found in [30]. The results show the maximum stress and principal strains stay below ultimate values. This indicates that the validation model with bone properties provides good structural rigidity as it would not fail under masticatory force of 120 lbs. It is also found that proper load transfer mechanism that resembles natural human skull buttress system can be attained. The detailed preparation and procedure of this validation process can be found in [38].

5 Conclusion

Reconstruction of facial deformity after cancer resection or serious injury is challenging. Not only, the characteristics of the on-site pathologies keep changing, but also bone goes through a constant remodeling with continuous adjustments due to stress changes. Thus, in order to develop a functional bone replacement, appropriate considerations of load, boundary, and time-dependent stress changes need to be incorporated. In this process, both the preoperative shape of the face and postoperative changes should be taken into consideration.

In this study, we have presented four different cases for mid-face craniofacial reconstruction where the bone replacements were designed using topology optimization. The cases have demonstrated the necessity of patient-specific solutions for craniofacial reconstruction and the effectiveness of topology-optimized solution. Realistic mastication simulation on 3D printed and FE model validates the feasibility of the solutions using experiments. The presented optimization technique is based on compliance (energy of deformation) minimization.

We would like to motivate to include the topology optimization procedure into the standard workflow of designing patient-specific bone implants. Patient presents with a craniofacial defect. From imaging modalities the data are registered, segmented, and truncated to achieve a working 3D model. The domain and the boundary conditions are extracted. A topology optimization procedure is performed to obtain the solution. The bone replacement design is then 3D printed and fused into the patient's 3D printed model. If required, a mechanical testing is performed to check the feasibility of the bone replacement. Once approved, the bone replacement shape can be used for the implant.

We are currently working on a multi-objective topology optimization framework that will incorporate porosity, multi-material, functionally-graded distribution, and biological variables (e.g., oxygen level in the replacement bone) [34, 38]. We have successfully demonstrated by means of mechanical testing that the bone replacement designs are feasible. Topology optimization offers great versatility in designing complicated bone replacements. This can be a new paradigm in bone tissue surgery and regeneration.

Acknowledgments This material is based upon work supported by the National Science Foundation under Grant No. 1032884. Diana Carrau was supported by the MD Student Research Fellowship from College of Medicine, Ohio State University.

References

- Adachi T, Osako Y, Tanaka M, Hojo M, Hollister SJ (2006) Framework for optimal design of porous scaffold microstructure by computational simulation of bone regeneration. *Biomaterials* 27(21):3964–3972
- Andrades P, Militsakh O, Hanasono MM, Rieger J, Rosenthal EL (2011) Current strategies in reconstruction of maxillectomy defects. *Arch Otolaryngol Head Neck Surg* 137(8):806–812
- Antony AK, Chen WF, Kolokythas A, Weimer KA, Cohen MN (2011) Use of virtual surgery and stereolithography-guided osteotomy for mandibular reconstruction with the free fibula. *Plast Reconstr Surg* 128(5):1080–1084
- Bandyopadhyay A, Espana F, Balla VK, Bose S, Ohgami Y, Davies NM (2010) Influence of porosity on mechanical properties and in vivo response of ti6al4v implants. *Acta Biomater* 6(4):1640–1648
- Bendsoe MP, Sigmund O (1999) Material interpolation schemes in topology optimization. *Arch Appl Mech* 69(9–10):635–654
- Bendsoe MP, Sigmund O (2003) *Topology optimization theory, methods and applications*. Springer, Berlin
- Bidra AS, Jacob RF, Taylor TD (2012) Classification of maxillectomy defects: a systematic review and criteria necessary for a universal description. *J Prosthet Dent* 107(4):261–270
- Bluebond-Langner R, Rodriguez ED (2009) Application of skeletal buttress analogy in composite facial reconstruction. *Cranio-maxillofac Trauma Reconstr* 2(1):19–25
- Cordeiro PG, Chen CM (2012) A 15-year review of midface reconstruction after total and subtotal maxillectomy: part II. technical modifications to maximize aesthetic and functional outcomes. *Plast Reconstr Surg* 129(1):139–147
- Cordeiro PG, Santamaria E (2000) A classification system and algorithm for reconstruction of maxillectomy and midfacial defects. *Plast Reconstr Surg* 105(7):2331–2346 (discussion 2347–8)
- Cypher TJ, Grossman JP (1996) Biological principles of bone graft healing. *J Foot Ankle Surg* 35(5):413–417
- Dalgorf D, Higgins K (2008) Reconstruction of the midface and maxilla. *Curr Opin Otolaryngol Head Neck Surg* 16(4):303–311
- Derand P, Rannar LE, Hirsch JM (2012) Imaging, virtual planning, design, and production of patient-specific implants and clinical validation in craniomaxillofacial surgery. *Cranio-maxillofac Trauma Reconstr* 5(3):137–144
- Dobbe JGG, Vroemen JC, Strackee SD, Streekstra GJ (2013) Patient-tailored plate for bone fixation and accurate 3d positioning in corrective osteotomy. *Med Biol Eng Comput* 51(1–2):19–27
- El-Hajje A, Kolos EC, Wang JK, Maleksaeedi S, He Z, Wiria FE, Choong C, Ruys AJ (2014) Physical and mechanical characterization of 3d-printed porous titanium for biomedical applications. *J Mater Sci Mater Med* 25(11):2471–2480
- Elsalanty ME, Genecov DG (2009) Bone grafts in craniofacial surgery. *Cranio-maxillofac Trauma Reconstr* 2(3):125–134
- Flint PW, Haughey BH, Lund VJ, Niparko JK, Richardson MA, Robbins KT, Thomas JR (2010) *Cummings otolaryngology—head and neck surgery*, 5th edn. Elsevier Health Sciences, Amsterdam
- Futran ND, Mendez E (2006) Developments in reconstruction of midface and maxilla. *Lancet Oncol* 7(3):249–258
- Genden EM (2010) Reconstruction of the mandible and the maxilla: the evolution of surgical technique. *Arch Facial Plast Surg* 12(2):87–90
- Gruss JS, Mackinnon SE (1986) Complex maxillary fractures: role of buttress reconstruction and immediate bone grafts. *Plast Reconstr Surg* 78(1):9–22
- Hanasono MM, Silva AK, Yu P, Skoracki RJ (2013) A comprehensive algorithm for oncologic maxillary reconstruction. *Plast Reconstr Surg* 131(1):47–60
- He Y, Zhu HG, Zhang ZY, He J, Sader R (2009) Three-dimensional model simulation and reconstruction of composite total

- maxillectomy defects with fibula osteomyocutaneous flap flow-through from radial forearm flap. *Oral Surg Oral Med Oral Pathol Oral Radiol Endod* 108(6):e6–e12
23. Hilloowala R, Kanth H (2007) The transmission of masticatory forces and nasal septum: structural comparison of the human skull and gothic cathedral. *Cranio* 25(3):166–171
 24. Hollister SJ (2009) Scaffold design and manufacturing: from concept to clinic. *Adv Mater* 21(32–33):3330–3342
 25. Hollister SJ, Maddox RD, Taboas JM (2002) Optimal design and fabrication of scaffolds to mimic tissue properties and satisfy biological constraints. *Biomaterials* 23(20):4095–4103
 26. Kang H, Lin CY, Hollister SJ (2010) Topology optimization of three dimensional tissue engineering scaffold architectures for prescribed bulk modulus and diffusivity. *Struct Multidiscipl Optim* 42(4):633–644
 27. Koolstra JH (2002) Dynamics of the human masticatory system. *Crit Rev Oral Biol Med* 13(4):366–376
 28. Manson PN, Hoopes JE, Su CT (1980) Structural pillars of the facial skeleton: an approach to the management of le fort fractures. *Plast Reconstr Surg* 66(1):54–62
 29. McCarthy CM, Cordeiro PG (2010) Microvascular reconstruction of oncologic defects of the midface. *Plast Reconstr Surg* 126(6):1947–1959
 30. McElhanev JH, Fogle JL, Melvin JW, Haynes RR, Roberts VL, Alem NM (1970) Mechanical properties of cranial bone. *J Biomech* 3(5):495
 31. Nagasao T, Nakajima T, Kimura A, Kaneko T, Jin H, Tamaki T (2005) The dynamic role of buttress reconstruction after maxillectomy. *Plast Reconstr Surg* 115(5):1328–1340 discussion 1341
 32. Neumann A, Kevenhoerster K (2009) Biomaterials for craniofacial reconstruction. *GMS Curr Top Otorhinolaryngol Head Neck Surg* 8:Doc08
 33. Nguyen TH, Paulino GH, Song J, Le CH (2010) A computational paradigm for multiresolution topology optimization (mtop). *Struct Multidiscipl Optim* 41(4):525–539
 34. Park J, Sutradhar A (2015) A multi-resolution method for 3d multi-material topology optimization. *Comput Methods Appl Mech Eng* 285:571–586
 35. Rudderman RH, Mullen RL (1992) Biomechanics of the facial skeleton. *Clin Plast Surg* 19(1):11–29
 36. Shen H, Brinson LC (2011) A numerical investigation of porous titanium as orthopedic implant material. *Mech Mater* 43(8):420–430
 37. Shen Y, Sun J, Li J, Li MM, Huang W, Ow A (2012) Special considerations in virtual surgical planning for secondary accurate maxillary reconstruction with vascularised fibula osteomyocutaneous flap. *J Plast Reconstr Aesthet Surg* 65(7):893–902
 38. Sutradhar A, Park J, Carrau D, Miller MJ (2014) Experimental validation of 3d printed patient-specific implants using digital image correlation and finite element analysis. *Comput Biol Med* 52:8–17
 39. Sutradhar A, Paulino GH, Miller MJ, Nguyen TH (2010) Topological optimization for designing patient-specific large craniofacial segmental bone replacements. *Proc Natl Acad Sci USA* 107(30):13222–13227
 40. Wang S, de Sturler E, Paulino GH (2007) Large-scale topology optimization using preconditioned Krylov subspace methods with recycling. *Int J Numer Methods Eng* 69(12):2441–2468

41. Yamamoto Y, Kawashima K, Sugihara T, Nohira K, Furuta Y, Fukuda S (2004) Surgical management of maxillectomy defects based on the concept of buttress reconstruction. *Head Neck* 26(3):247–256

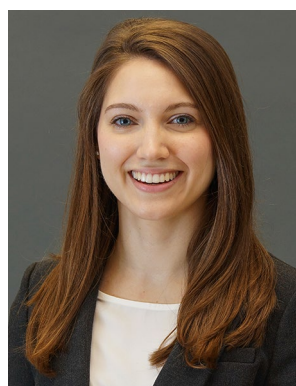


Alok Sutradhar received his Ph.D. in civil engineering with specialization in computational mechanics and computational science from the University of Illinois at Urbana-Champaign in 2005. After graduation, he started as a postdoctoral fellow in MD Anderson Cancer center working on surgery simulation. Later, he continued as a post-doctoral researcher at the Department of Surgery at The Ohio State University working on biomedical modeling and craniofacial bone replacements.

In 2011, he joined the Department of Plastic Surgery at The Ohio State University (OSU) as an assistant professor. He is also a faculty in the Department of Mechanical and Aerospace Engineering at OSU. His research interests include computational surgery, computational biomechanics, bioinspired-optimized design, biomimetic material and biomedical modeling.



Jaeyong Park received his M.S. in Mechanical Engineering from the Ohio State University in 2013. He is currently in the Ph.D. program in the same academic institute with expected graduation in 2016. His main research interests include structural engineering, computational mechanics and optimization techniques for multidisciplinary problems.



Diana Carrau received her M.D. from The Ohio State University in 2015, where she continues her training as a plastic surgery resident. Her research interests lie within the areas of pediatric and adult craniofacial reconstruction.



Tam H. Nguyen received his Ph.D. in civil engineering from the University of Illinois at Urbana Champaign in 2010. He is a Postdoctoral Research Associate in the Department of Civil and Environmental Engineering, Northeastern University. His research interests include fracture mechanics, craniofacial reconstruction, reliability-based design and topology optimization.



Glaucio H. Paulino holds the ‘Raymond Allen Jones’ Chair at the Georgia Institute of Technology. From 2009 to 2011, he was director of the ‘Mechanics of Materials’ program and also the acting director of the ‘Nano and Biomechanics’ program at the National Science Foundation. His research interests include computational mechanics, development of methodologies to characterize the deformation and fracture behavior of existing and emerging materials and structural systems, and

topology optimization for large-scale multiscale/multiphysics problems.



Michael J. Miller is Professor of Surgery and Chair of the Department of Plastic Surgery at The Ohio State University. He is a highly sought after reconstructive surgeon, educator and investigator. His research interests include regenerative medicine and advanced technology applications in clinical surgery.